

Multi-Modal Few-Shot Temporal Action Detection

Sauradip Nag^{1,5} Mengmeng Xu^{2,4*} Xiatian Zhu^{1,3} Juan-Manuel Pérez-Rúa²
Bernard Ghanem⁴ Yi-Zhe Song^{1,5} Tao Xiang^{1,5}

¹ CVSSP, University of Surrey, UK ² Meta, UK ³ Surrey Institute for People-Centred Artificial Intelligence, UK

⁴ KAUST, Saudi Arabia ⁵ iFlyTek-Surrey Joint Research Center on Artificial Intelligence, UK

Abstract

Few-shot (FS) and zero-shot (ZS) learning are two approaches for scaling temporal action detection (TAD) to new classes. The former adapts a pretrained vision model to a new task represented by as few as a single video per class, whilst the latter requires no training examples by exploiting a semantic description of the new class. In this work, we introduce a new multi-modality few-shot (MMFS) TAD problem, as a marriage of FS-TAD and ZS-TAD by leveraging few-shot support videos and a new class name jointly. To tackle this problem, we further introduce a novel **M**ulti-modality **P**rompt **m**ETa-learning (MUPPET) method. This is enabled by efficiently bridging pretrained vision and language models whilst maximally reusing already learned capacity. Concretely, we construct multi-modal prompts by mapping support videos into the textual token space of a vision-language model using a meta-learned adapter-equipped visual semantics tokenizer. To tackle large intra-class variation, we further design a query feature regulation scheme. Extensive experiments on ActivityNetv1.3 and THUMOS14 demonstrate that our MUPPET outperforms state-of-the-art alternative methods, often by a large margin. MUPPET can be easily extended to few-shot object detection, achieving new state-of-the-art on MS-COCO. The code will be made available in <https://github.com/sauradip/MUPPET>

1. Introduction

The objective of temporal action detection (TAD) is to predict the temporal duration (*i.e.*, start and end time) and the class label of each action instance in an untrimmed video [16, 4]. Conventional TAD methods [44, 45, 3, 40, 54, 28, 27] are based on supervised learning, requiring many (*e.g.*, hundreds) videos per class with costly segment-level annotations for training. This thus severely limits their ability to scale to many classes. To alleviate this problem, few-shot (FS) [47, 48, 51, 30] and zero-shot (ZS)

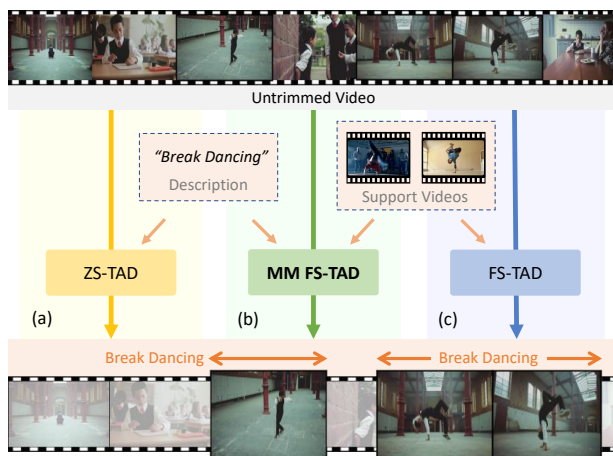


Figure 1. **Illustration of different problem settings.** (a) *Zero-shot temporal action detection* (ZS-TAD) represents a new class using a semantic description of its name (*i.e.*, textual input). (c) *Few-shot temporal action detection* (FS-TAD) can learn a new class from a few support (training) videos (*i.e.*, visual input). (b) Our new *multimodal few-shot temporal action detection* (MMFS-TAD) can leverage both textual and visual inputs.

[51, 18, 29] learning based TAD methods have been recently introduced.

Specifically, FS-TAD aims to learn a model that can adapt to new action classes with as few as a single training video per class (Fig. 1(c)). This is achieved often by meta-learning a TAD model over a distribution of simulated tasks on seen classes. ZS-TAD further removes the need for any training samples from new classes. Instead, new classes are represented by projecting their class names into some semantic space (*e.g.*, attributes, word embeddings), (Fig. 1(a)). Once the semantic space is aligned with a visual feature space, a model trained on seen classes can be applied/transferred to new ones. The recent emergence of large-scale Visual-Language (ViL) models (*e.g.*, CLIP [32] and ALIGN [17]) have clearly advanced the research of *zero-shot learning* in general, and ZS-TAD in particular [18, 29]. This is because these ViL models offer a strong alignment between the text (*e.g.*, action class name or de-

*This work was done while internship in Meta,UK

scription) and visual (*e.g.*, video content features) modalities, which is a key requirement for ZS-TAD.

FS-TAD and ZS-TAD have thus far been studied *independently*. This is in contrast to the object classification/detection domain where attempts have been made to unify the two problems in a single framework [15, 11]. Tackling them jointly in TAD makes sense for a number of reasons. (1) These two problems have a shared goal of scaling up TAD. (2) In practice, one often has a few examples of a new class, together with the class name. (2) The two tasks are complementary to one another, *e.g.*, the semantic description extracted from an action name can compensate for the limitation of few-shot examples in representing the large intra-class variations in action. One of the potential obstacles with this unification is that the semantic description from an action name is often too weak to describe the rich visual context of that action, and therefore cannot match with the representation power of even a single video example [1]. However, this has been changed with the ever-stronger ViL models available, as mentioned above.

In this work, for the first time, TAD is studied under a new setting, namely *multimodal few-shot temporal action detection* (MMFS-TAD), characterized by learning from both support videos (*i.e.*, visual modality) and class names (*i.e.*, textual modality). More specifically, we introduce a novel *Multi-Modality Prompt Meta-Learning* (MUPPET) method to efficiently fuse few-shot visual examples and high-level class semantic text information. Grounded on a pre-trained vision-language (ViL) model (*e.g.*, CLIP), MUPPET integrates meta-learning with learning-to-prompt in a unified TAD framework. This is made possible by introducing a *multimodal prompt learning module* that maps the support videos of a novel task into the textual token space of the ViL model using a meta-learned adapter-equipped visual semantics tokenizer. During meta-training, this tokenizer is jointly learned with other components in order to map visual representations into a designated $\langle context \rangle$ token compatible with the language model. During inference (*i.e.*, meta-test), given a new task, our model can induce by digesting few training examples and class names in a data-driven manner. With the ViL’s text encoder, our multimodal prompt can be then transformed to multimodal class prototypes for action detection. To tackle the large intra-class challenge due to limited support samples, we design a query feature regulation strategy by meta-learning a masking representation from the support sets and attentive conditioning.

We summarize our **contributions** as follows. (1) We propose the multimodal few-shot temporal action detection (MMFS-TAD) problem. (2) To solve this new problem, we introduce a novel *Multi-Modality Prompt Meta-Learning* (MUPPET) method that integrates meta-learning and learning-to-prompt in a single formulation. It can be

easily plugged into existing TAD architectures and is flexible in tackling FS-TAD and ZS-TAD either independently or jointly. (3) To better relate query videos with limited support samples, we design a query feature regulation scheme based on meta-learning a masking representation from the support sets, and attentive conditioning. (4) Extensive experiments on ActivityNet-v1.3 and THUMOS14 validate the superiority of our MUPPET over state-of-the-art alternative methods in the MMFS-TAD, ZS-TAD, and FS-TAD settings. Under minimal adaptation, MUPPET can also achieve superior few-shot object detection performance on COCO.

2. Related Works

Temporal action detection Substantial progress has been made in TAD. Inspired by object detection [34], R-C3D [43] uses anchor boxes in the pipeline of proposal generation and classification. Similarly, TURN [12] aggregates local features to represent snippet features for temporal boundary regression and classification. SSN [54] decomposes an action instance into start:course:end and employs structured temporal pyramid pooling for proposal generation. BSN [23] generates proposals with high start and end probabilities by modeling the start, end, and actionness at each time. Later, BMN [22] improves the actionness by generating a boundary-matching confidence map. For better proposal generation, G-TAD [45] learns semantic and temporal context via graph convolutional networks. CSA [36] enriches the proposal temporal context via attention transfer. Unlike most previous models adopting a sequential localization and classification pipeline, TAGS [28] introduces a different design with parallel localization and classification based on a notion of global segmentation masking. All the above methods are supervised with reliance on large training data, and thus less scalable.

Few-shot temporal action detection By fast adaptation of a model to any given new class with few training samples, few-shot learning (FSL) provides a solution for scalability [39, 37, 35]. FSL is often realized by meta-learning which simulates new tasks with novel classes represented by only a handful of labeled samples. FSL has been introduced to TAD in [47], by incorporating sliding window in a matching network [39] strategy. Later on, [51] consider weak video-level annotation of untrimmed training videos. [49] performed few-shot spatio-temporal action detection with a focus on a single new class at a time. Recently, [30] used the Transformer for adapting the support learned features to the query features in untrimmed videos.

Zero-shot temporal action detection Alternatively, zero-shot learning allows for recognizing new classes with no labeled training data. This line of research has advanced significantly due to the promising power of large vision-language (ViL) models, *e.g.*, CLIP trained by 400 million

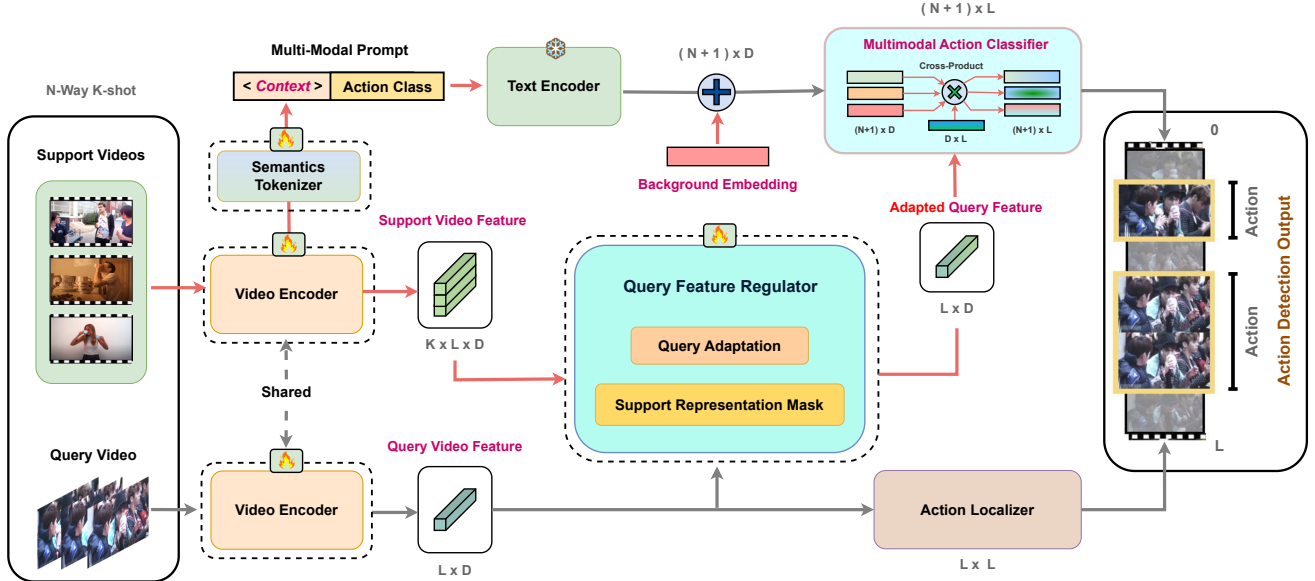


Figure 2. **Overview of our Multi-Modality Prompt Meta-Learning (MUPPET) method.** We adopt the global mask-based TAD architecture [28, 29]. The key components of MUPPET include (1) multimodal prompt meta-learning (Sec. 3.2) and (2) query feature regulation (Sec. 3.3). Dotted-line boxes represent the meta-learned modules.

image-text pairs [32]. Follow-ups further boost the zero-shot transferable ability, *e.g.*, CoOp [55], CLIP-Adapter [13], and Tip-adapter [53]. In video domains, a similar idea has also been explored for transferable representation learning [25], and text-based action localization [31]. CLIP is used recently in action recognition [41] and TAD [18, 29].

In this work, FS-TAD and ZS-TAD are unified in a new MMFS-TAD setting. Our MUPPET can tackle either FS-TAD or ZS-TAD, and crucially both simultaneously when both visual examples and class descriptions are available.

3. Methodology

3.1. Preliminaries: Multi-Modal Few-Shot

We establish the proposed multimodal few-shot learning by integrating class semantic information (*e.g.*, text such as action class names) to few-shot learning [8]. To facilitate understanding, we follow the standard episode-based meta-learning convention. Given a new task in each episode with a few labeled support videos per unseen class (*i.e.*, visual modality) and class names (*i.e.*, textual modality), we aim to learn a TAD model for that task. For a N -way K -shot setting, the support set S consists of K labeled samples for each of the N action classes. The query set Q has a single sample per class. Key to MMFS-TAD is to leverage limited video examples and action class names jointly. We have a base class set C_{base} for training, and a novel class set C_{novel} for test. For testing cross-class generalization, we ensure they are disjoint: $C_{base} \cap C_{novel} = \phi$. The base and novel sets are denoted as $D_{base} = \{(V_i, Y_i), Y_i \in C_{base}\}$ and $D_{novel} = \{(V_i, Y_i), Y_i \in C_{novel}\}$ respectively. Under the proposed

setting, each training video V_i is associated with segment-level annotation $Y_i = \{(s_t, e_t, c), t \in \{1, \dots, M\}, c \in C\}$ including M segment labels each with the start and end time and action class c . In evaluation, for each task, we randomly sample a set of classes $L \sim C_{novel}$ each with the support set S (K videos) and the query set Q (one video) respectively. The labels of S are accessible for few-shot learning whilst that of Q is only used for performance evaluation.

As illustrated in Fig. 2, our *Multi-Modality Prompt Meta-Learning* (MUPPET) model consists of a video encoder, a meta-mapper, a text encoder, a query regulator and decoder heads.

3.2. Multi-Modal Prompt Learning

Given a few training videos with a class name, we design a meta-learning process for multi-modal fusion in prompts. As shown in Fig. 3, we extract each video’s feature with a video encoder and project it into the textual token space with a visual semantics tokenizer. The class name is then encoded by the text tokenizer [13] and further concatenated to the visual tokens. We apply a text encoder to create the multi-modal prompt embedding. Let us describe the video encoder, visual semantics tokenizer, and text encoder next.

Video encoder We employ a residual adapter θ on a pre-trained Vision-Transformer (ViT) [5] to learn the video priors. Since the training data in TAD is relatively small due to costly labeling, using adapter facilitates the reuse of pretrained knowledge during fine-tuning. Formally, an untrimmed video is encoded into a feature tensor $V \in \mathbb{R}^{3 \times T \times H \times W}$ with T frames and a spatial resolution of

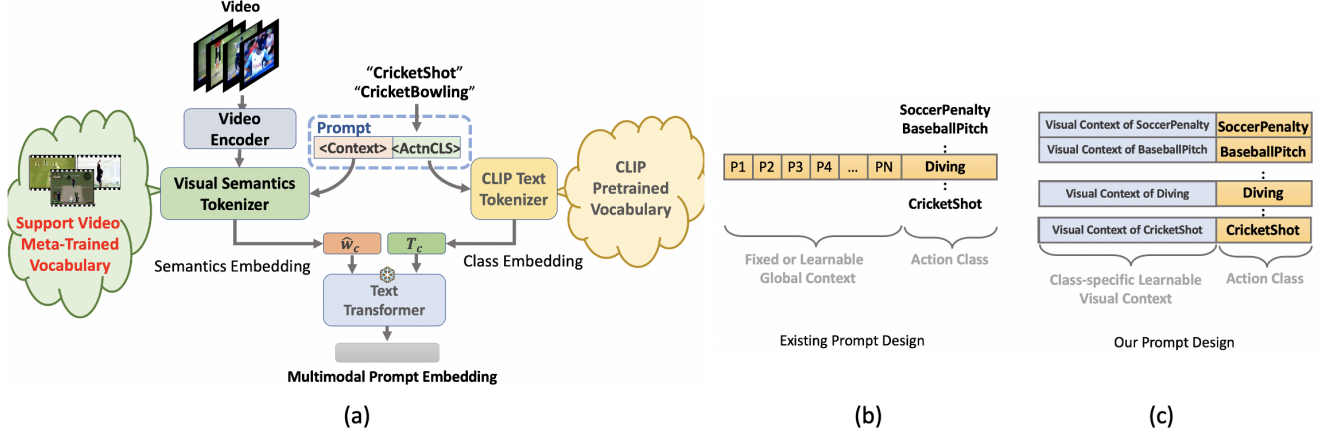


Figure 3. **Multimodal prompt meta-learning.** (a) We meta-learn a visual semantics tokenizer for translating the support videos (*i.e.*, visual modality) to the textual token space of a pretrained ViL model. Together with the tokens of class names, this mapping facilitates the creation of multimodal prompts using the pretrained text encoder. (b) Unlike previous class-generic visual prompts, we consider more discriminative class-specific counterparts.

$H \times W$. To capture global context information useful for modeling long-term dependency, another light transformer ϕ is applied to the time dimension:

$$F = \mathbb{V}(V; [\theta, \phi]) \in \mathbb{R}^{t \times D}, \quad (1)$$

where D is the snippet feature dimension and t is the number of temporal snippets. Then, following [22, 46], we uniformly sample L equidistant features over all the t snippets to obtain the video feature $E \in \mathbb{R}^{D \times L}$. Finally, given a K -shot task $T_i = \{S_i, Q_i\}$, we extract the support features $E_s \in \mathbb{R}^{K \times D \times L}$ for S_i and query features $E_q \in \mathbb{R}^{D \times L}$ for Q_i . More details are given in Supplementary.

Visual semantics tokenizer Multi-modal learning requires the interaction across modalities in a common space. To that end, we propose a visual semantics tokenizer f_{θ_s} based on set Transformer [21] as:

$$\hat{w}_c = f_{\theta_s}(\hat{E}_s^k | k = 1, 2, \dots, K) \in W, \quad (2)$$

where θ_s is the parameters, and \hat{E}_s^k is the action/foreground feature of support videos, which are obtained by trimming off the background frame features of E_s . W is the textual token space. Concretely, we set the query/key/value of f_{θ_s} all to \hat{E}_s^k so that the token \hat{w}_c predicted by the visual feature w.r.t. the designated learnable $\langle context \rangle$ token (see Fig. 3(a)) is learned to be compatible with the textual embeddings in W .

Text encoder The text encoder processes a text sequence and outputs a feature distribution. It has a text tokenizer $\psi \in \mathbb{R}^D$ that maps each token of the input into a representation space. Instead of learning a common prompt embedding for all the target classes as [55] (Fig. 3(b)), we propose to learn a *class-specific context embedding* (Fig. 3(c)) for generating more discriminative new class representation

(Table 3). We obtain the class token embeddings $T_c = \psi(c)$ using the pretrained language model tokenizer, then concatenate it with the $\langle context \rangle$ token embedding \hat{w}_c from the visual semantics tokenizer to form a multimodal prompt: $\hat{p} = [\hat{w}_c][T_c]$. In doing so, we can leverage the ViL model’s text transformer $\mathbb{T}()$, denoted as

$$\hat{z}_c = \mathbb{T}(\hat{p}) \in \mathbb{R}^{C \times D}, \quad (3)$$

to obtain the multi-modal representation \hat{z}_c with both visual (support videos) and textual (class names) modalities jointly encoded for action class c .

For TAD, a background class is needed which however is lacking from the vocabulary of ViL model. To solve this, we learn a specific background embedding $\hat{z}_{bg} \in \mathbb{R}^D$ with random initialization. We append this to \hat{z}_c , yielding a complete multimodal representation $E_{mm} \in \mathbb{R}^{(C+1) \times D}$.

3.3. Query Feature Regulator

As shown in the middle of Fig. 2, we also design a transformer-based query regulator in parallel with multi-modal prompt learning. This regulator takes as input the features from support video and query video, and it facilitates the association of action instances across support and query videos in the same action class, with typically large differences (*i.e.*, large intra-class variation). Inspired by representation masking [29] for suppressing background, we also introduce a representation masking mechanism as shown in Fig. 4, which uses the support masked feature for query adaptation.

Representation masking We start with this masking using a transformer decoder \mathcal{S} . Given per-class temporal features of a query video $E_q \in \mathbb{R}^{D \times L}$, we project that to \mathbb{N}_q query embeddings \mathcal{Q} . Cross-attended with the support video features $E_s \in \mathbb{R}^{K \times D \times L}$, we generate \mathbb{N}_q latent embeddings,

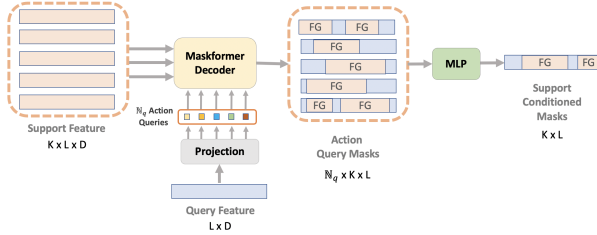


Figure 4. Support conditioned representation masking.

followed by a mask projection to obtain H as:

$$H = \mathcal{S}(E_s, Q; \theta_m) \in \mathbb{R}^{N_q \times K \times L}, \quad (4)$$

where θ_m are the trainable parameters of \mathcal{S} . H represents the most-probable foreground masks in the support videos. To obtain a single mask per location $\hat{H} \in \mathbb{R}^{K \times L}$, a tiny MLP for 1D masking is employed. This support video mask is then binarized yielding the foreground mask \hat{H}_{bin} . The support masked representation E_s^{fg} is obtained by applying \hat{H}_{bin} on E_s . This masking is trained on the support videos with ground truth and applied to the query videos to obtain the support masked features.

Query feature regulation We use the support masked feature for regularizing the query feature by cross-attention. Specifically, with a transformer encoder \mathcal{C} , we set the query video feature as its query \mathbb{Q} , and the support masked feature as its key \mathbb{K} and value \mathbb{V} . As the number of support videos per class varies, we aggregate \mathbb{K} and \mathbb{V} by averaging over the number of shots to match a query video. We then concatenate \mathbb{K}/\mathbb{V} with the query feature to form an enhanced version \mathbb{K}_{agg} and \mathbb{V}_{agg} . The query feature is finally regulated via $\bar{E}_q = \mathcal{C}(E_q, \mathbb{K}_{agg}, \mathbb{V}_{agg}; \theta_q)$ where θ_q is a learnable parameter.

3.4. TAD Classifier and Localizer Heads

We adopt the TAD head design of [29, 28] with parallel classification and mask prediction.

Multimodal classifier The output of the query feature regulator is fed to the classifier head. We exploit $\hat{E}_{mm} \in \mathbb{R}^{(C+1) \times D}$ as a multimodal classifier to classify the regulated query features $\bar{E}_q \in \mathbb{R}^{L \times D}$ as:

$$\mathcal{P} = \rho((\hat{E}_{mm} * (\bar{E}_q)^T) / \tau) \in \mathbb{R}^{(C+1) \times L}, \quad (5)$$

where each column of \mathcal{P} is the classification result $p_l \in \mathbb{R}^{(C+1) \times 1}$ of each snippet $t \in L$, $\tau = 0.7$ is a temperature coefficient and ρ denotes the softmax function.

Action mask localizer In parallel to classification, this stream predicts 1D binary masks of action instances over the whole video. We use a stack of 1D dynamic-convolution layers to form the mask classifier \mathbb{H} . Specifically, given t -th snippet $\bar{E}_q(t)$, it outputs a 1D mask $m_t = [q_1, \dots, q_L] \in$

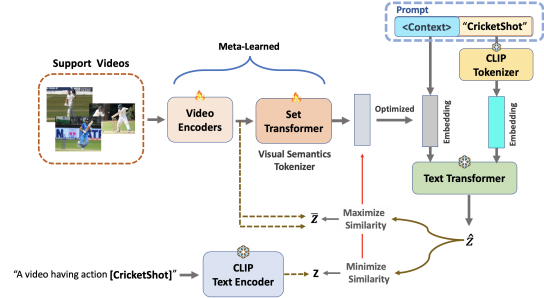


Figure 5. **Multi-modal prompt optimization:** Given a set of support video examples of an action class and its label (“Cricket Shot”), we embed them with the meta-learned video encoder and predict an embedding using the visual semantics tokenizer f_{θ_s} . We then further tune the embedding with a contrastive loss \mathcal{L}_{tok} $\mathbb{R}^{L \times 1}$ with each $q_i \in [0, 1] (i \in [1, L])$ meaning the action probability at i -th snippet. We define it formally:

$$\mathcal{M} = \sigma(\mathbb{H}(E_q), \theta_l), \quad (6)$$

where σ is a sigmoid activation and t -th column of \mathcal{M} is the mask prediction by t -th snippet and θ_l is the learnable parameter.

3.5. Meta Training and Inference

Learning objective Following [29], we adopt the cross-entropy loss \mathcal{L}_c for classification, binary dice loss \mathcal{L}_m and binary mask loss \mathcal{L}_{comp} for masking. For more effective training, we further impose a contrastive criterion [6] to optimize the visual semantics tokenizer (Fig. 5). Given the multimodal representation \hat{z}_c , original prompt embedding z_c , and video embedding \bar{z}_c for each class c , the contrastive loss is defined as:

$$\mathcal{L}_{tok} = -\log \frac{\exp(\cos(\bar{z}_c, \hat{z}_c))}{\exp(\cos(\bar{z}_c, \hat{z}_c)) + 2 \exp(\cos(z_c, \hat{z}_c))}, \quad (7)$$

where $\cos(\cdot)$ is cosine similarity and the factor 2 is for contrasting z_c with both visual and textual embeddings. To contrast background (z_{bg}) from foreground (\hat{z}_c), we minimize:

$$\mathcal{L}_{bg} = \operatorname{argmin} \sum_{j=1}^C (\cos(z_{bg}, z_c^j) - \delta_{bg})^2, \quad (8)$$

where δ_{bg} is the margin hyper-parameter.

Training The training procedure has two stages. In the **first** stage, the model is trained on the base dataset D_{base} in a standard supervised learning manner. More specifically, we deploy the objective $\mathcal{L}_{base} = \mathcal{L}_c + \mathcal{L}_m + \mathcal{L}_{comp} + \mathcal{L}_{tok} + \mathcal{L}_{bg} + \mathcal{L}_{const}$ and optimize the parameter set $\phi_{base} = \{\theta, \phi, \theta_s, \theta_m, \theta_q, \theta_l\}$. This trains all modules of MUPPET except the language model end-to-end. The **second** stage is for few-shot fine-tuning, following a typical meta-learning paradigm. Due to no ground-truth for query

Method		N-way	Modality		ActivityNetv1.3				THUMOS14			
			Visual	Text	0.5	0.75	0.95	Avg	0.3	0.5	0.7	Avg
FS	FS-Trans	1	✗	✗	42.2	24.8	5.2	25.6	42.6	25.7	8.2	25.5
	QAT				44.6	26.4	4.9	26.9	38.7	24.4	7.5	24.3
	MUPPET				45.4	28.1	5.6	27.8	44.1	26.2	8.5	26.1
	Feat-RW	5			30.7	16.6	2.9	17.1	35.3	19.6	6.8	20.1
	Meta-DETR				32.9	20.3	4.6	19.4	37.5	20.7	7.5	21.9
FSVOD	34.5		18.9	5.1	21.6	37.9	23.8	7.3	22.8			
MUPPET	36.9	22.2	5.9	23.0	41.2	25.7	8.5	24.9				
MMFS	OV-DETR	1	✗	✓	44.2	27.9	6.3	28.7	46.1	29.7	9.0	30.4
	Owl-Vit				43.7	27.0	6.0	27.2	45.2	29.0	9.0	30.2
	EffPrompt				45.9	27.9	5.2	29.4	47.2	30.4	9.8	31.1
	STALE				47.7	29.3	7.6	30.3	48.9	32.1	10.3	32.0
	Baseline-I				46.9	28.6	6.9	29.7	47.3	30.5	9.2	31.8
	MUPPET	49.7	32.9		9.2	32.7	50.6	33.5	11.2	33.8		
	OV-DETR	5	✗		39.8	22.3	5.4	23.1	40.4	23.9	7.5	24.0
	Owl-Vit				37.9	20.3	5.6	21.9	38.3	21.9	7.7	22.6
	EffPrompt				41.1	21.6	5.4	23.8	39.5	23.5	7.6	24.8
	STALE				42.3	22.9	6.8	24.5	40.7	24.9	7.1	25.4
Baseline-I	42.1			22.7	6.0	24.0	40.2	24.7	7.0	25.0		
MUPPET	45.3	25.6	6.3	26.2	42.3	27.2	7.8	27.5				
ZS	EffPrompt	All	✗	32.0	19.3	2.9	19.6	37.2	21.6	7.2	21.9	
	STALE		✗	32.1	20.7	5.9	20.5	38.3	21.2	7.0	22.2	
	Baseline-I		✓	30.6	18.0	4.1	18.7	35.8	20.5	7.1	20.8	
	MUPPET		✗	33.5	21.9	6.7	22.0	40.1	22.8	8.1	24.8	

Table 1. Comparing our MUPPET with prior art few-shot (FS), zero-shot (ZS) and alternative methods. *Setting*: 5-shot; the CLIP model for multimodal few-shot (MMFS) methods; 50%/50% train/test class split for all ZS methods.

videos under this setting, we freeze the query regularizer (θ_q^{base}) and action localizer head (θ_l^{base}). We thus minimize $\phi_{meta} = \{\theta, \phi, \theta_s, \theta_m\}$, with \mathcal{L}_m and \mathcal{L}_c removed. More details on meta-learning is given in Supplementary.

Inference At test time, we generate action instance predictions for each query video by the classification \mathbf{P} and mask \mathbf{M} predictions following [29]. For each top scoring action snippet in \mathbf{P} , we then obtain the temporal masks by thresholding the corresponding column of \mathbf{M} using a set of thresholds $\Theta = \{\theta_i\}$. We apply SoftNMS [2] to obtain the final top-scoring outputs.

4. Experiments

Datasets We evaluate two popular TAD benchmarks. (1) ActivityNet-v1.3 [4] has 19,994 videos from 200 action classes. We follow the standard split setting of 2:1:1 for train/val/test. (2) THUMOS14 [16] has 200 validation videos and 213 testing videos from 20 categories with labeled temporal boundary and action class.

Settings We consider two major settings. *Few-shot setting*: To facilitate fair comparison, we adopt the same dataset and class split as [30]. For both datasets, we divide all the classes into three non-overlapping subsets for training (80%), validation (10%), and testing (10%), respectively. The validation set is used for model parameter tuning and best model selection. We consider 1-way/class and 5-way settings. We consider naturally untrimmed sup-

port videos. For each N -way K -shot experiment, we divide the base and novel class videos into few-shot episodes where each episode consists of $N \times (K + 1)$ tasks. We train with 1000 episodes and test with 250 episodes with random tasks and report the average result. *Zero-shot setting*: In this setting, similar to few-shot, we ensure that $D_{val} \cap D_{test} = \phi$. We follow the setting and dataset splits used by [29] for a fair comparison. For both datasets, we train with 50% classes and test on 50% classes. To ensure statistical significance, we conduct 10 random samplings to split classes for each setting, following [18]. More details on splits are provided in Supplementary.

Implementation details For a fair comparison, we use CLIP [32] initialized weights for both datasets. For comparing with CLIP-based TAD baselines, we use the image and text encoders from pretrained CLIP (ViT-B/16+Transformer) [32]. We also used Kinetics [20] pretrained initialization for showing the robustness of our approach. Video frames are pre-processed to 112×112 in spatial resolution, and the maximum number of textual tokens is 77, following CLIP. Given a variable-length video, we first sample every 6 consecutive frames as a snippet. Then we feed the snippet into our vision encoder and extract the features before the fully connected layer. Thus, we obtain a sequence of snippet-level feature for the untrimmed video. After this, each video’s feature sequence F is rescaled to $T = 100/256$ snippets for Ac-

tivityNet/THUMOS using linear interpolation. Our model is trained on 6 NVIDIA 3090RTX GPUs with 1000/250 episodes using Adam optimizer with a learning rate of $10^{-4}/10^{-5}$ for ActivityNet/THUMOS respectively during base and meta-training. More implementation details are provided in Supplementary.

4.1. Comparison with state-of-the-art

Competitors We consider extensively three sets of previous possible methods: **(1) Few-shot learning based** methods: Two action detection methods (FS-Trans [49] and QAT [30]). AS FS-Trans was originally designed for spatiotemporal action detection, we discarded the spatial detection part here. Due to limited FS-TAD models, we adapt 2 object detection baselines (Feat-RW [19], Meta-DETR [52]). We replaced their backbones with CLIP ViT encoders and the object decoders with TAD decoders. We similarly adapted a video-based object detection method (FSVOD [9]) where temporal action proposals and temporal matching network are applied with TAD decoder. For a fair comparison, we deploy MUPPET in the FS setting by discarding the textual input. **(2) Multi-modal Few-shot learning based** methods: As this is a new problem, we need to adapt existing methods for baselines. We adapted zero-shot object detection methods (OV-DETR [50], OWL-ViT [26]) as they can facilitate the multi-modal setting due to their CLIP based design. For [50], we kept the encoder unchanged for frame-level extraction and replaced the decoder with a start/end regressor as RTD-Net [38]. For [26], we used the encoder backbone unchanged and replaced the bounding box detectors with a start/end regressor as BMN [22]. We also considered two TAD methods (EffPrompt [18] and STALE [29]) by finetuning all modules with support set during inference. We further adapted zero-shot classification method CoCOOP [56] (denoted as *Baseline-I*) to zero-shot TAD model STALE [29] by adding the meta-network from visual branch to learn the textual tokens. This is the closest competitor of our proposed MUPPET. **(3) Zero-shot learning based** methods: EffPrompt [18] and STALE [29] and *Baseline-I*. We deploy MUPPET in ZS setting by discarding the FS components (*e.g.*, visual-semantics tokenizer and query regularizer). All the methods use the same CLIP ViT [32] vision encoders for a fair comparison.

Results We make several observations from the results in Table 1. **(1) FS setting:** Even with 1-way support sets, FS-TAD methods (FS-Trans [49], QAT [30]) still outperform 5-way object detection based counterparts (Feat-RW [19], Meta-DETR [52], FSVOD [9]). This indicates the importance of modeling temporal dynamics and task-specific design. Our MUPPET outperforms the 1/5-way alternatives by 0.9/1.4% margin verifying the superiority of our model design. **(2) MMFS setting:** Interestingly, object detection methods (OV-DETR [50], OWL-ViT [26]) can perform

similarly as FS-TAD (EffPrompt [18], STALE [29]) ones when using text modality. Our *Baseline-I* yields competitive performance. Notably, MUPPET surpasses the best FS-TAD model (QAT) by a margin of 5.8%, validating the superiority of our model and our motivation for MMFS-TAD. In particular, QAT tackles 1-way FS-TAD (*i.e.*, foreground class vs. background) similar to action proposal generation. The result suggests that our multimodal classifier is better than the popular UntrimmedNet. A similar observation can be drawn in the 5-way case. **(3) ZS setting:** Our MUPPET is superior to recent art models (EffPrompt [18], STALE [29]) and *Baseline-I* (an integrated model even using training videos). This verifies the flexibility of our method in deployment, in addition to promising performance.

4.2. Ablation Studies

MMFS vs. FS setting MUPPET by the design choice can work in both few-shot setting (by removing the language encoder) and multi-modal few-shot setting. To examine the usefulness of textual semantic information, we compare the result under the 5-way 5-shot setting on ActivityNet. As shown in Table 2, with MUPPET a gain of 3.2% can be benefited from the class semantic description. This validates our motivation that text modality can compensate for the limited few-shot examples.

Table 2. MUPPET in 5-way 5-shot setting on ActivityNet.

Setting	Text	0.5	0.75	0.95	Avg
FS	✗	36.9	22.2	5.9	23.0
MMFS	✓	45.3	25.6	6.3	26.2

Table 3. Prompt learning design on ActivityNet. Setting: 5-way.

Design	Shots	Prompt style		mAP	
		Learnable	Context	0.5	Avg
LPS	-	✗	-	18.4	13.6
LVP	5	✓	Visual	43.2	25.0
LTP	5	✓	Text	42.7	24.7
Ours	1	✓	Visual	43.7	25.1
Ours	5	✓	Visual	45.3	26.2

Prompt learning design We evaluate our multimodal prompt meta-learning that meta-learns the semantic information from few-shot support videos. We compare it against three alternatives: (i) *Learnable Prompt from Scratch (LPS)*: Learning the prompt from random vectors without the text encoder of ViL model (CLIP [32] in this case). (ii) *Learnable Textual Prompt (LTP)*: Learning the prompt from randomly initialized vectors with the text encoder of ViL model. (iii) *Learnable Visual Prompt (LVP)*: Learning the prompt from vectors initialized by visual features from the visual encoder of ViL model, as *Baseline-I*. We observe from Table 3 that: **(1) Lever-**

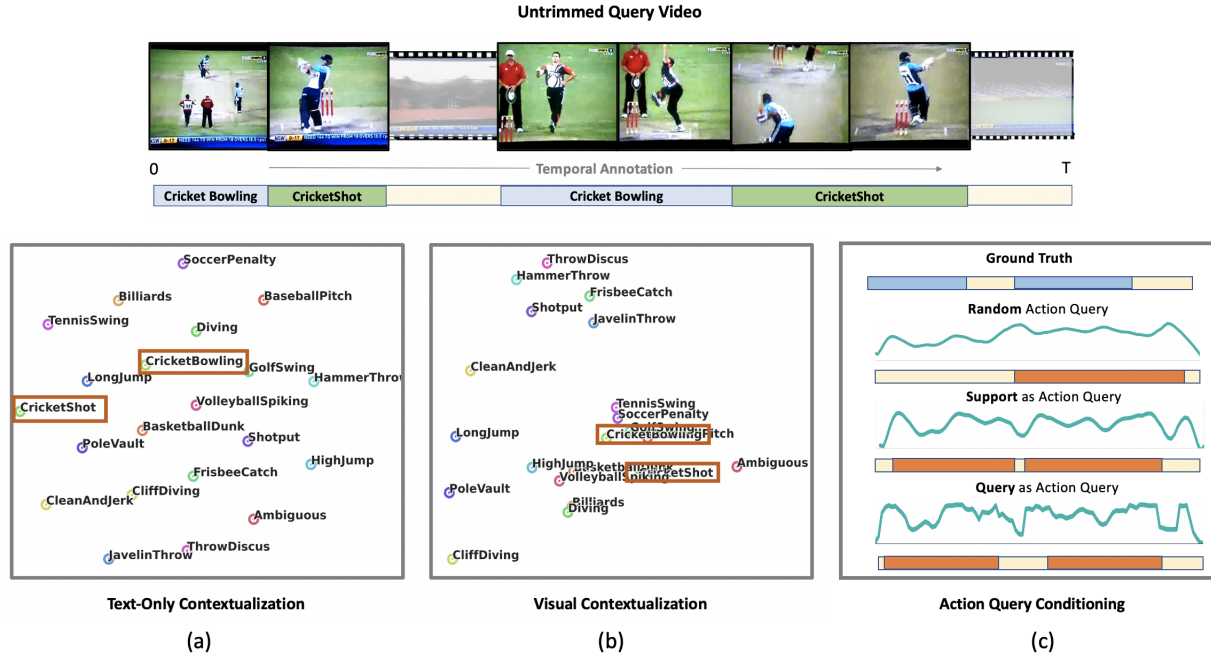


Figure 6. **Illustration of the impact of MUPPET on a random video** (a) PCA plot of our model with textual prompts (b) PCA plot of our model after incorporating visual semantics (c) Impact of various action query initialization method on actionness of representation mask.

aging the pretrained text encoder is critical due to pretraining on vast training data, otherwise, a big drop would occur as demonstrated by LPS. (2) Learning from only few visual samples via a meta-network, LVP is inferior to our MUPPET, verifying the complementary effect of our semantics tokenizer. (3) However, using only text modality for prompt learning (*i.e.*, LTP) is even inferior to visual modality only (*i.e.*, LVP). This is not surprising as videos provide more comprehensive and finer information about new classes. This effect is indicated in Fig. 7 that visual information helps in grouping similar actions such as “making an omelet” and “preparing salad”. (4) Also, the inferiority of LTP and LVP to ours suggests that learning class-specific tokens as we design is more suitable than learning a set of global prompts shared for all classes in MMFS-TAD.

We further examine the network choice (1D CNN *vs.* set Transformer [21]) for visual semantics tokenizer, and the necessity of class-specific prompts. As shown in Table 4, we see that: (1) A permutation invariant set Transformer is better than 1D CNN. (2) Using a single token per class is enough by our prompting method. This is different from previous prompting methods [55] that instead learn multiple (*e.g.*, 20) global tokens shared by all classes.

Episodic adapters in video encoder We exploit episodic adapters for the video encoder of ViL model. Alternative methods include (i) *Freezing video encoder* without any task adaptation as STALE [29], (ii) *Fine-tuning* the video encoder. We also compare with the adapted STALE for MMFS-TAD. We observe from Table 5 that: (1) Fine-tuning

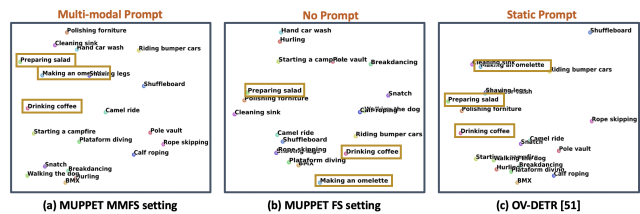


Figure 7. PCA of classifier weights on ActivityNet. As highlighted in the boxes, it is evident that visual information is useful in grouping related actions such as “preparing salad” and “making an omelet” so that the embedding space is made more meaningful. Best viewed when zoom-in.

is indeed useful as expected, as compared to the frozen encoder. However, it is less effective due to limited training data. (2) Using our adapters is the best which alleviates overfitting with higher efficiency by only learning a fraction of the parameters.

Table 4. Design of visual semantics tokenizer on ActivityNet. Setting: 5-way 5-shot. #T/C: Tokens per Class.

Network	Meta-Learn	#T/C	mAP	
			0.5	Avg
1D CNN	✗	20	37.4	21.3
	✓	20	40.8	23.0
	✓	1	39.7	22.5
Set Transformer [21]	✗	1	43.8	24.7
	✓	1	45.3	26.2
	✓	20	44.7	25.6

Query feature regulation MMFS-TAD often presents a large intra-class variation due to limited training video data. Our query feature regulation is designed for overcoming

Table 5. Video encoder on ActivityNet. Setting: 5-way 5-shot.

Method	Video encoder	mAP	
		0.5	Avg
MUPPET	Freeze	41.1	25.3
	Full-tuning	45.0	26.1
	Adapters	45.3	26.2

Table 6. Query feature regulation on ActivityNet. Setting: 5-way.

K-shot	Query Masking	mAP	
		0.5	Avg
-	✗	41.1	24.8
1	✓	43.7	25.1
5	✓	45.3	26.2

Table 7. Representation masking on support video features on ActivityNet. Setting: 5-way 5-shot.

Masking decoder	Initialization	mAP	
		0.5	Avg
1D CNN	-	31.7	21.3
MaskFormer [7]	Random	38.2	24.9
	Support	43.7	25.8
	Query	45.3	26.2

this challenge. As shown in Table 6, this scheme is effective with the gain increasing along with the shots of the training set. This validates the usefulness of our design. In Table 7 we observe a gain of 1.3% in mAP@0.5. We also show that randomly initialization leads to inferior foreground prediction (see Fig 6(c)). Support video features based initialization can improve but still not as strong as query video features as in our design.

Ablation of visual adapter: We have ablated the role of adapters in feature backbone in Tab 8. For this experiment, we compared two previous ViT based baselines *Baseline-1* and STALE [29]. The residual adapters are plugged into the ViT backbone maintaining the same configuration with MUPPET. From the results in Tab 8, it is evident that the variant with adapter improves the performance, however, MUPPET w/o adapter variant is still stronger than the adapter infused baselines. This suggests the superiority of our model design.

Table 8. MUPPET in 5-way 5-shot setting on ActivityNet

Method	Backbone	0.5	0.75	0.95	Avg
Baseline-1	w/Adapter	42.5	23.0	6.0	24.2
STALE	w/ Adapter	42.7	23.2	6.9	24.7
MUPPET	w/o Adapter	45.0	25.2	6.0	26.1
	w/ Adapter	45.3	25.6	6.3	26.2

Ablation with different pretraining We experiment our MUPPET with Kinetics-400 pretraining. Concretely, we use Kinetics-400 pretrained weights for both visual and textual branch provided by ActionCLIP [41] in this experiment. From Table 9 we observe similar findings as that

of CLIP [32] pretrained features in Table 1 (Main paper). Our MUPPET outperforms the competitors by similar margin and better than CLIP pretraining by 4% in avg mAP. This confirms that the superiority of our method is feature agnostic, with the desired capability of reducing the domain gap between pretraining and downstream tasks.

Table 9. Analysis of MUPPET with different pre-training feature on ActivityNet in 5-way 5-shot setting.

Method	Feature	mAP			
		0.5	0.75	0.95	Avg
EffPrompt	CLIP	41.1	21.6	5.4	23.8
STALE	CLIP	42.3	22.9	6.8	24.5
MUPPET	CLIP	45.3	25.6	6.3	26.2
MUPPET	K-400	48.1	29.4	10.0	30.2

4.3. Multi-modal Few-shot Object Detection

For generality evaluation, we further adapt MUPPET to MMFS object detection. We replace the video-encoder with ViT+adapter [32] image encoder and TAD decoder with object classifier and bounding-box regressor. More details can be found in Supplementary. Experiments are conducted on COCO [24], following the same MMFS setup as in TAD. From Table 10 it is observed that the multi-modal information is indeed beneficial in few-shot object detection surpassing the nearest competitor META-DETR [52] by 0.5%/1.1% in 5/10-shot setting. This suggests that our method can favorably serve as a unified framework for both object and action detection under the multimodal few-shot setting.

Table 10. Comparing our adapted MUPPET with existing few-shot object detection methods on COCO dataset.

Method	5-Shot			10-Shot		
	AP	AP ₅₀	AP ₇₅	AP	AP ₅₀	AP ₇₅
FRCN [33]	4.6	8.7	4.4	5.5	10.0	5.5
TFA w/ cos [42]	7.0	13.3	6.5	9.1	17.1	8.8
Deform-DETR [57]	7.4	12.3	7.7	11.7	19.6	12.1
FSOD [10]	-	-	-	12.0	22.4	11.8
QA-FewDet [14]	9.7	20.3	8.6	11.6	23.9	9.8
META-DETR [52]	15.4	25.0	15.8	19.0	30.5	19.7
MUPPET	15.9	26.4	14.8	20.1	32.3	19.9

5. Conclusions

In this work, we have presented a *multi-modality few-shot temporal action detection* (MMFS-TAD) problem setting that tackles the conventional FS-TAD and ZS-TAD jointly. We further proposed a novel *Multi-modality Prompt meta-learning* (MUPPET) method, characterized by prompt meta-learning from multimodal inputs, adapters-based ViL model adaptation, and query feature regulation. Extensive experiments on two benchmarks show that our MUPPET surpasses both strong baselines and state-of-the-art methods under a variety of settings. We also show the

generic superiority of our method in tackling multi-modal few-shot object detection.

References

- [1] George Awad, Jonathan Fiscus, David Joy, Martial Michel, Alan F Smeaton, Wessel Kraaij, Maria Eskevich, Robin Aly, Roeland Ordelman, Marc Ritter, et al. Trecvid 2016: Evaluating video search, video event detection, localization, and hyperlinking. In *TREC Video Retrieval Evaluation (TRECVID)*, 2016. 2
- [2] Navaneeth Bodla, Bharat Singh, Rama Chellappa, and Larry S Davis. Soft-nms—improving object detection with one line of code. In *Proceedings of the IEEE international conference on computer vision*, pages 5561–5569, 2017. 6
- [3] Shyamal Buch, Victor Escorcia, Chuanqi Shen, Bernard Ghanem, and Juan Carlos Niebles. Sst: Single-stream temporal action proposals. In *CVPR*, 2017. 1
- [4] Fabian Caba Heilbron, Victor Escorcia, Bernard Ghanem, and Juan Carlos Niebles. Activitynet: A large-scale video benchmark for human activity understanding. In *CVPR*, pages 961–970, 2015. 1, 6
- [5] Shoufa Chen, Chongjian Ge, Zhan Tong, Jiangliu Wang, Yibing Song, Jue Wang, and Ping Luo. Adaptformer: Adapting vision transformers for scalable visual recognition. *arXiv preprint arXiv:2205.13535*, 2022. 3
- [6] Ting Chen, Simon Kornblith, Mohammad Norouzi, and Geoffrey Hinton. A simple framework for contrastive learning of visual representations. 2020. 5
- [7] Bowen Cheng, Alexander G. Schwing, and Alexander Kirillov. Per-pixel classification is not all you need for semantic segmentation. 2021. 9
- [8] Xuanyi Dong, Liang Zheng, Fan Ma, Yi Yang, and Deyu Meng. Few-example object detection with model communication. *TPAMI*, 41(7), 2018. 3
- [9] Qi Fan, Chi-Keung Tang, and Yu-Wing Tai. Few-shot video object detection. *arXiv preprint arXiv:2104.14805*, 2021. 7
- [10] Qi Fan, Wei Zhuo, Chi-Keung Tang, and Yu-Wing Tai. Few-shot object detection with attention-rpn and multi-relation detector. In *Proceedings of the IEEE/CVF Conference on Computer Vision and Pattern Recognition*, pages 4013–4022, 2020. 9
- [11] Yanwei Fu, Timothy M Hospedales, Tao Xiang, and Shao-gang Gong. Transductive multi-view zero-shot learning. *IEEE transactions on pattern analysis and machine intelligence*, 37(11):2332–2345, 2015. 2
- [12] Jiyang Gao, Zhenheng Yang, Kan Chen, Chen Sun, and Ram Nevatia. Turn tap: Temporal unit regression network for temporal action proposals. In *ICCV*, 2017. 2
- [13] Peng Gao, Shijie Geng, Renrui Zhang, Teli Ma, Rongyao Fang, Yongfeng Zhang, Hongsheng Li, and Yu Qiao. Clip-adapter: Better vision-language models with feature adapters. *arXiv preprint arXiv:2110.04544*, 2021. 3
- [14] Guangxing Han, Yicheng He, Shiyuan Huang, Jiawei Ma, and Shih-Fu Chang. Query adaptive few-shot object detection with heterogeneous graph convolutional networks. In *Proceedings of the IEEE/CVF International Conference on Computer Vision*, pages 3263–3272, 2021. 9
- [15] Guangxing Han, Jiawei Ma, Shiyuan Huang, Long Chen, Rama Chellappa, and Shih-Fu Chang. Multimodal few-shot object detection with meta-learning based cross-modal prompting. *arXiv preprint arXiv:2204.07841*, 2022. 2
- [16] Haroon Idrees, Amir R Zamir, Yu-Gang Jiang, Alex Gorban, Ivan Laptev, Rahul Sukthankar, and Mubarak Shah. The thumos challenge on action recognition for videos “in the wild”. *Computer Vision and Image Understanding*, 155:1–23, 2017. 1, 6
- [17] Chao Jia, Yinfei Yang, Ye Xia, Yi-Ting Chen, Zarana Parekh, Hieu Pham, Quoc Le, Yun-Hsuan Sung, Zhen Li, and Tom Duerig. Scaling up visual and vision-language representation learning with noisy text supervision. In *International Conference on Machine Learning*, pages 4904–4916. PMLR, 2021. 1
- [18] Chen Ju, Tengda Han, Kunhao Zheng, Ya Zhang, and Weidi Xie. A simple baseline on prompt learning for efficient video understanding. 2022. 1, 3, 6, 7
- [19] Bingyi Kang, Zhuang Liu, Xin Wang, Fisher Yu, Jiashi Feng, and Trevor Darrell. Few-shot object detection via feature reweighting. In *ICCV*, 2019. 7
- [20] Will Kay, Joao Carreira, Karen Simonyan, Brian Zhang, Chloe Hillier, Sudheendra Vijayanarasimhan, Fabio Viola, Tim Green, Trevor Back, Paul Natsev, et al. The kinetics human action video dataset. *arXiv preprint arXiv:1705.06950*, 2017. 6
- [21] Juho Lee, Yoonho Lee, Jungtaek Kim, Adam R Kosiorek, Seungjin Choi, and Yee Whye Teh. Set transformer. In *International Conference on Machine Learning*, 2019. 4, 8
- [22] Tianwei Lin, Xiao Liu, Xin Li, Errui Ding, and Shilei Wen. Bmn: Boundary-matching network for temporal action proposal generation. In *Proceedings of the IEEE/CVF International Conference on Computer Vision*, pages 3889–3898, 2019. 2, 4, 7
- [23] Tianwei Lin, Xu Zhao, Haisheng Su, Chongjing Wang, and Ming Yang. BSN: Boundary sensitive network for temporal action proposal generation. In *ECCV*, 2018. 2
- [24] Tsung-Yi Lin, Michael Maire, Serge Belongie, James Hays, Pietro Perona, Deva Ramanan, Piotr Dollár, and C Lawrence Zitnick. Microsoft coco: Common objects in context. In *European conference on computer vision*, pages 740–755. Springer, 2014. 9
- [25] Antoine Miech, Jean-Baptiste Alayrac, Lucas Smaira, Ivan Laptev, Josef Sivic, and Andrew Zisserman. End-to-end learning of visual representations from uncurated instructional videos. In *Proceedings of the IEEE/CVF Conference on Computer Vision and Pattern Recognition*, pages 9879–9889, 2020. 3
- [26] Matthias Minderer, Alexey Gritsenko, Austin Stone, Maxim Neumann, Dirk Weissenborn, Alexey Dosovitskiy, Aravindh Mahendran, Anurag Arnab, Mostafa Dehghani, Zhuoran Shen, et al. Simple open-vocabulary object detection with vision transformers. *arXiv preprint arXiv:2205.06230*, 2022. 7
- [27] Sauradip Nag, Xi Tian Zhu, Yi-Zhe Song, and Tao Xiang. Temporal action localization with global segmentation mask transformers. 2021. 1

- [28] Sauradip Nag, Xiatian Zhu, Yi-zhe Song, and Tao Xiang. Proposal-free temporal action detection via global segmentation mask learning. In *ECCV*, 2022. 1, 2, 3, 5
- [29] Sauradip Nag, Xiatian Zhu, Yi-zhe Song, and Tao Xiang. Zero-shot temporal action detection via vision-language prompting. In *ECCV*, 2022. 1, 3, 4, 5, 6, 7, 8, 9
- [30] Sauradip Nag, Xiatian Zhu, and Tao Xiang. Few-shot temporal action localization with query adaptive transformer. *arXiv preprint arXiv:2110.10552*, 2021. 1, 2, 6, 7
- [31] Sudipta Paul, Niluthpol Chowdhury Mithun, and Amit K Roy-Chowdhury. Text-based localization of moments in a video corpus. *IEEE Transactions on Image Processing*, 30:8886–8899, 2021. 3
- [32] Alec Radford, Jong Wook Kim, Chris Hallacy, Aditya Ramesh, Gabriel Goh, Sandhini Agarwal, Girish Sastry, Amanda Askell, Pamela Mishkin, Jack Clark, et al. Learning transferable visual models from natural language supervision. In *International Conference on Machine Learning*, pages 8748–8763. PMLR, 2021. 1, 3, 6, 7, 9
- [33] Shaoqing Ren, Kaiming He, Ross Girshick, and Jian Sun. Faster r-cnn: Towards real-time object detection with region proposal networks. *Advances in neural information processing systems*, 28, 2015. 9
- [34] Shaoqing Ren, Kaiming He, Ross Girshick, and Jian Sun. Faster r-cnn: towards real-time object detection with region proposal networks. *TPAMI*, 39(6):1137–1149, 2016. 2
- [35] Jake Snell, Kevin Swersky, and Richard S Zemel. Prototypical networks for few-shot learning. *arXiv preprint arXiv:1703.05175*, 2017. 2
- [36] Deepak Sridhar, Niamul Quader, Srikanth Muralidharan, Yaoxin Li, Peng Dai, and Juwei Lu. Class semantics-based attention for action detection. In *Proceedings of the IEEE/CVF International Conference on Computer Vision*, pages 13739–13748, 2021. 2
- [37] Flood Sung, Yongxin Yang, Li Zhang, Tao Xiang, Philip HS Torr, and Timothy M Hospedales. Learning to compare: Relation network for few-shot learning. In *CVPR*, 2018. 2
- [38] Jing Tan, Jiaqi Tang, Limin Wang, and Gangshan Wu. Relaxed transformer decoders for direct action proposal generation. In *Proceedings of the IEEE/CVF International Conference on Computer Vision (ICCV)*, pages 13526–13535, October 2021. 7
- [39] Oriol Vinyals, Charles Blundell, Timothy Lillicrap, Koray Kavukcuoglu, and Daan Wierstra. Matching networks for one shot learning. *arXiv preprint arXiv:1606.04080*, 2016. 2
- [40] Limin Wang, Yuanjun Xiong, Dahua Lin, and Luc Van Gool. Untrimmednets for weakly supervised action recognition and detection. In *CVPR*, pages 4325–4334, 2017. 1
- [41] Mengmeng Wang, Jiazheng Xing, and Yong Liu. Actionclip: A new paradigm for video action recognition. *arXiv preprint arXiv:2109.08472*, 2021. 3, 9
- [42] Xin Wang, Thomas E Huang, Trevor Darrell, Joseph E Gonzalez, and Fisher Yu. Frustratingly simple few-shot object detection. *arXiv preprint arXiv:2003.06957*, 2020. 9
- [43] Huijuan Xu, Abir Das, and Kate Saenko. R-c3d: Region convolutional 3d network for temporal activity detection. In *ICCV*, 2017. 2
- [44] Mengmeng Xu, Juan-Manuel Perez-Rua, Xiatian Zhu, Bernard Ghanem, and Brais Martinez. Low-fidelity end-to-end video encoder pre-training for temporal action localization. In *NeurIPS*, 2021. 1
- [45] Mengmeng Xu, Chen Zhao, David S Rojas, Ali Thabet, and Bernard Ghanem. G-tad: Sub-graph localization for temporal action detection. In *CVPR*, 2020. 1, 2
- [46] Mengmeng Xu, Chen Zhao, David S. Rojas, Ali Thabet, and Bernard Ghanem. G-tad: Sub-graph localization for temporal action detection. In *CVPR*, June 2020. 4
- [47] Hongtao Yang, Xuming He, and Fatih Porikli. One-shot action localization by learning sequence matching network. In *CVPR*, 2018. 1, 2
- [48] Pengwan Yang, Vincent Tao Hu, Pascal Mettes, and Cees GM Snoek. Localizing the common action among a few videos. In *ECCV*. Springer, 2020. 1
- [49] Pengwan Yang, Pascal Mettes, and Cees GM Snoek. Few-shot transformation of common actions into time and space. In *Proceedings of the IEEE/CVF Conference on Computer Vision and Pattern Recognition*, pages 16031–16040, 2021. 2, 7
- [50] Yuhang Zang, Wei Li, Kaiyang Zhou, Chen Huang, and Chen Change Loy. Open-vocabulary detr with conditional matching. *arXiv preprint arXiv:2203.11876*, 2022. 7
- [51] Da Zhang, Xiyang Dai, and Yuan-Fang Wang. Metal: Minimum effort temporal activity localization in untrimmed videos. In *CVPR*, 2020. 1, 2
- [52] Gongjie Zhang, Zhipeng Luo, Kaiwen Cui, and Shijian Lu. Meta-detr: Few-shot object detection via unified image-level meta-learning. *arXiv preprint arXiv:2103.11731*, 2(6), 2021. 7, 9
- [53] Renrui Zhang, Rongyao Fang, Peng Gao, Wei Zhang, Kunchang Li, Jifeng Dai, Yu Qiao, and Hongsheng Li. Tip-adapter: Training-free clip-adapter for better vision-language modeling. *arXiv preprint arXiv:2111.03930*, 2021. 3
- [54] Yue Zhao, Yuanjun Xiong, Limin Wang, Zhirong Wu, Xiaou Tang, and Dahua Lin. Temporal action detection with structured segment networks. In *ICCV*, 2017. 1, 2
- [55] Kaiyang Zhou, Jingkang Yang, Chen Change Loy, and Ziwei Liu. Learning to prompt for vision-language models. *arXiv preprint arXiv:2109.01134*, 2021. 3, 4, 8
- [56] Kaiyang Zhou, Jingkang Yang, Chen Change Loy, and Ziwei Liu. Conditional prompt learning for vision-language models. In *Proceedings of the IEEE/CVF Conference on Computer Vision and Pattern Recognition*, pages 16816–16825, 2022. 7
- [57] Xizhou Zhu, Weijie Su, Lewei Lu, Bin Li, Xiaogang Wang, and Jifeng Dai. Deformable detr: Deformable transformers for end-to-end object detection. *arXiv preprint*, 2020. 9